Check for updates

How to cite: *Angew. Chem. Int. Ed.* **2024**, *63*, e202319810
doi.org/10.1002/anie.202319810

Polymer Chemistry | Hot Paper

Ring-Opening Terpolymerisation of Elemental Sulfur Waste with Propylene Oxide and Carbon Disulfide via Lithium Catalysis

*Cesare Gallizioli, David Battke, Helmut Schlaad, Peter Deglmann, and Alex J. Plajer**

Abstract: Elemental sulfur, a waste product of the oil refinement process, represents a promising raw material for the synthesis of degradable polymers. We show that simple lithium alkoxides facilitate the polymerisation of elemental sulfur S_8 with industrially relevant propylene oxide (PO) and CS_2 (a base chemical sourced from waste S_8 itself) to give poly(monothiocarbonate-alt-S_x) in which x can be controlled by the amount of supplied sulfur. The in situ generation of thiolate intermediates obtained by a rearrangement, which follows CS_2 and PO incorporation, allows to combine S_8 and epoxides into one polymer sequence that would otherwise not be possible. Mechanistic investigations reveal that alkyl oligosulfide intermediates from S_8 ring opening and sulfur chain length equilibration represent the better nucleophiles for inserting the next PO if compared to the trithiocarbonates obtained from the competing CS_2 addition, which causes the sequence selectivity. The polymers can be crosslinked in situ with multifunctional thiols to yield reprocessable and degradable networks. Our report demonstrates how mechanistic understanding allows to combine intrinsically incompatible building blocks for sulfur waste utilisation.

Introduction

Sulfur-containing polymers have shown promise as redox and light responsive, sensorics as well as chemically recyclable materials with improved thermal and optical properties as compared to their non-sulfurated counterparts.[1–11] In the societal context, it is beneficial to access these directly from S_8, which is a megaton scale waste product of the petrochemical industry from oil refining (Figure 1 **(a)**), or from high sulfur-wt % base chemicals sourced from S_8 such as carbon disulfide CS_2.[12,13] Consequently, a great deal of effort is currently concerned with the synthesis of useful polymeric materials from S_8 itself or chemicals directly sourced from S_8.[14–17] For example, many crosslinked polymers have been synthesised in recent years through *inverse vulcanisation* which have found numerous applications as lenses, electrodes, elastomers, heavy metal scavengers and reprocessable thermosets.[18–22,22–26] Although linear thermoplastics can be prepared via different (typically polycondensation) methods, these often require expensive or highly reactive reagents, only incorporate low amounts of sulfur or yield oligomers.[27] Given the cyclic structure of S_8, one might imagine that ring-opening polymerisation would be suitable to produce polysulfur S_n, however this process is thermodynamically unfavourable at ambient condition (floor temperature 159 °C) and requires copolymerisation techniques to obtain stable polymers.[28]

In this regard, Penczek and Duda (Figure 1 **(b^1)**) reported in the late 1970s that S_8 undergoes ring-opening copolymerisation (ROCOP) with thiiranes under $CdCO_3$ or NaSPh@18-crown-6 catalysis to form polysulfide of the type $[-CR_2\text{-}CH_2\text{-}S_x-]_n$ (R = H, Me; x = 1–9).[23–25] Ren et al. very recently expanded this approach to $PPNSbF_6$/MTBD catalysis to selectively yield polydisulfides.[26] In both cases the key to S_8 activation was that thiirane ring opening leads to a thiolate intermediate, which can open the S_8 ring under formation of an anionic oligosulfide and then propagates. Again, these methodologies depend on the use of expensive or even non-commercial thiiranes. It would be much more attractive to be able to copolymerise S_8 with the lighter homologous of thiiranes, namely epoxides, as some of these, e.g. propylene oxide PO, are large scale industrial chemicals.[32,33] Unfortunately, epoxides do not copolymerise with S_8 as the metal-alkoxide intermediates formed from epoxide ring opening does not form stable intermediate or links with S_8 (Figure 1**(b^2)**).[34] However if one could generate thiolate intermediates in epoxide polymerisations their copolymerisation with S_8 could be achieved. In this regard, Komber and Werner et al. reported that the lithium alkoxide-catalysed ROCOP of CS_2/PO yields poly(monothio-*alt*-trithiocarbonate)s (i.e. –O–C(=S)–O– or "OSO" groups in alternation with –S–C(=S)–S– or "SSS" groups, Figure 1 **(b^3)**) rather than poly(dithiocarbonate)s

[*] C. Gallizioli, A. J. Plajer
Makromolekulare Chemie I, Universität Bayreuth, Universitätsstraße 30, 95447 Bayreuth
E-mail: alex.plajer@uni-bayreuth.de
D. Battke
Institut für Chemie und Biochemie, Freie Universität Berlin, Fabeckstraße 34–36, 14195 Berlin
H. Schlaad
Institute für Chemie, Universität Potsdam, Karl-Liebknecht-Straße 24–25, 14476 Potsdam
P. Deglmann
BASF SE, Carl-Bosch-Straße 38, 67056 Ludwigshafen am Rhein

© 2024 The Authors. Angewandte Chemie International Edition published by Wiley-VCH GmbH. This is an open access article under the terms of the Creative Commons Attribution License, which permits use, distribution and reproduction in any medium, provided the original work is properly cited.

© 2024 The Authors. Angewandte Chemie International Edition published by Wiley-VCH GmbH

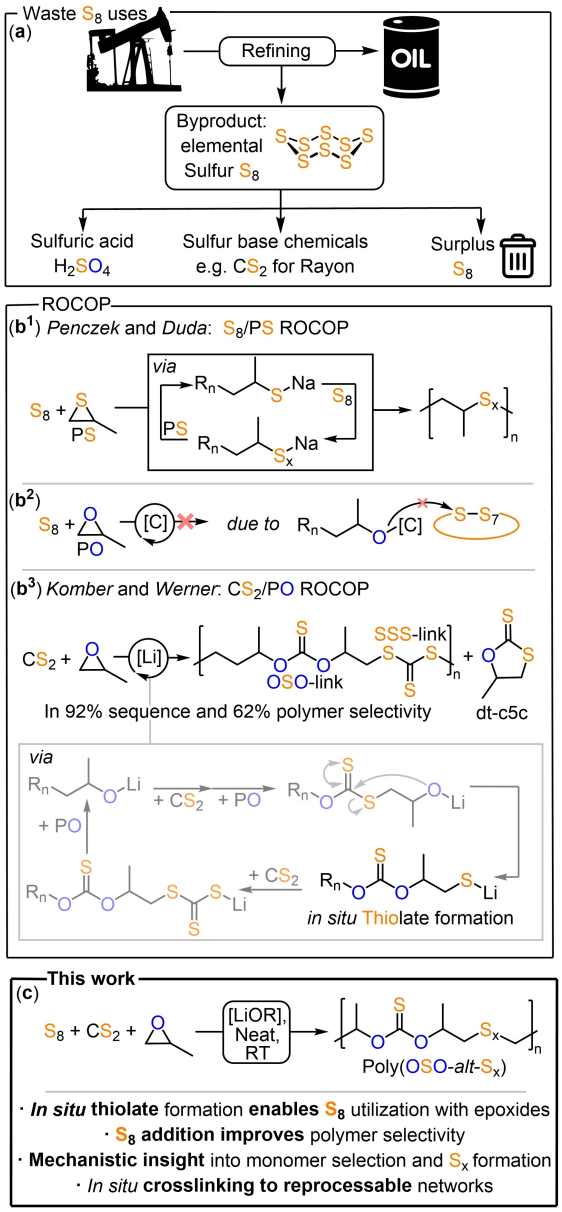

Figure 1. (a) Conceptual Scheme concerning the production and use of S_8. (b^1) Ring-opening copolymerisation (ROCOP) of S_8 with propylene sulfide (PS) via thiolate intermediates. (b^2) Alkoxide intermediates from propylene oxide (PO) ring-opening prevent S_8/PO ROCOP; [C] denotes catalyst, R_n denotes polymer chain. (b^3) In situ thiolate formation during CS_2/PO ROCOP. (c) Key finding of the presented work.

with –O–C(C=S)–S– or "OSS" links.[35] The polymers show an unusual head-to-head-*alt*-tail-to-tail sequence in that the tertiary "head" CH groups from PO ring opening sits next to OSO links and secondary "tail" CH_2 groups sits next to SSS links. The sequence can be rationalised by an O/S exchange process at the chain end transforming lithium alkoxides into lithium thiolate intermediates and it is commonplace, albeit rarely controlled in the ROCOP of epoxides and oxetanes with sulfurated comonomers.[36–43] Accordingly, we hypothesised that these thiolates might be capable of activating S_8 to allow polymer formation from epoxides, S_8 and CS_2 which we report in this contribution.

Results and discussion

In an initial attempt to achieve S_8/CS_2/PO ring-opening terpolymerisation (ROTERP) at room temperature, we tested the polymerisation with 1 eq. lithium benzyl oxide (LiOBn, generated from $Li[N(SiMe_3)_2]$ and BnOH, see ESI Section S2), 250 eq. PO, 500 eq. CS_2 and 125 eq. S (i.e. 1/8 S_8) (Table 1 run #1). Aliquot analysis of the product mixture after 3 h by ^{1}H NMR spectroscopy revealed the emergence of indicative broad resonances at 5.80–5.40 ppm, corresponding to CH protons from ring-opened PO adjacent to OSO groups, and 3.50–2.80 ppm, corresponding to CH_2 adjacent to S_x groups (verified by Raman spectroscopy, see below) (Figure 2**(a)**); these resonances can be tentatively assigned in reference to the copolymers produced by ROCOP of CS_2/PO and S_8/PS.[31,44] In addition to formation of 84 % polymer (i.e., polymer selectivity is 84 %), we also obtained approximately 16 % cyclic five-membered propylene dithiocarbonate (dt-c5c) by-product; this can be easily removed from the crude reaction mixture by precipitation from DCM/MeOH. 2D NMR spectroscopy of the isolated polymer showed tertiary carbons ($\delta(C^t) = 78$ ppm) bound to OSO ($\delta(C^q) = 193$ ppm) links and secondary carbons ($\delta(C^s) = 43$ ppm) adjacent to S_x links. Hence the copolymer exhibits a poly(OSO-*alt*-S_x) microstructure in head-to-head-*alt*-tail-to-tail regioselectivity, which is reminiscent of the poly(OSO-*alt*-SSS) structure described by Komber and Werner et al. with S_x in place of trithiocarbonate links.[35] The selectivity of OSO and S_x versus other links (e.g. dithio- OSS and trithiocarbonate SSS) is 98 %. No (thio)ether links could be observed. Note that during this process H_2S evolution did not occur, which otherwise is a common problem in other S_8 copolymerisations.[45] GPC analysis reveals an apparent weight-average molar mass of the copolymer of $M_w = 20$ kDa ($Đ = 1.7$). The copolymer is obtained as yellow semi-solid, due to the presence of the C=S chromophore. It is soluble in common organic solvents such as THF, benzene or $CHCl_3$ and can be hot-pressed into optically clear films (Figure 2(a)). The material features a high refractive index of 1.58 due to the high molar refractivity of the sulfur centres present in the polymer chain.

Moving to different sulfur loadings (Table 1, run #2–#5) showed that polymer and sequence selectivity positively correlate with the amount of supplied S_8 in the starting monomer feed. Very high sequence selectivity of > 98 % and polymer selectivity of > 90 % could be achieved. Note that the lithium-alkoxide catalysed ROCOP of CS_2/PO in the absence of S_8 gave a decreased polymer selectivity of ca. 60 %.[35] This is particularly dramatic at a higher reaction temperature of 80 °C, for which ROTERP (run #6) gave 90 % polymer selectivity while ROCOP of CS_2/PO (run #7) produced no copolymer but only cyclic dithiocarbonate. Near quantitative polymer selectivity is even observed at 120 °C for the ROTERP (run #8) albeit with reduced linkage

© 2024 The Authors. Angewandte Chemie International Edition published by Wiley-VCH GmbH

15213773, 2024, 17, Downloaded from https://onlinelibrary.wiley.com/doi/10.1002/anie.202319810 by Universitaet Bayreuth, Wiley Online Library on [03/10/2024]. See the Terms and Conditions (https://onlinelibrary.wiley.com/terms-and-conditions) on Wiley Online Library for rules of use; OA articles are governed by the applicable Creative Commons License

Table 1: Reaction conditions and molecular characteristics of the polymers obtained by ROTERP of S_8/CS_2/PO.

Run	LiOBn:PO:CS_2:$^1/_8S_8$	T [°C]	t [h]	Conv. [%][a]	Polymer [%][b]	Disulfide [%][c]	Linkage [%][d]	M_w [kDa][e]	$Đ$[e]
#1	1:250:250:125	RT	3	96	84	70	98	20	1.7
#2	1:250:250:250	RT	4	99	89	44	97	28	1.7
#3	1:250:250:500	RT	4	99	91	24	97	27	1.7
#4	1:250:250:1000	RT	3	94	92	15	93	25	1.5
#5	1:250:250:90	RT	4	100	72	89	92	17	1.7
#6	1:250:250:250	80	1	81	89	46	87	5	1.5
#7	1:250:250:0	80	1	99	0	–	–	–	–
#8	1:250:250:250	120	0.17	99	97	18	80	7	1.5
#9	1:250:500:250	RT	16	99	90	33	95	28	1.6
#10	1:250:750:125	RT	4	94	77	73	94	19	1.6
#11	1:250:500:500	RT	2	73	90	25	96	27	1.8
#12	1:250:500:1000	RT	2	79	89	20	98	20	1.8
#13	1:1000:1000:500	RT	72	99	85	69	94	45	1.5
#14	1:2000:2000:1000	RT	26	98	83	66	97	43	1.5
#15[f]	1:400:0:400	RT	24	73	–	–	–	24	1.6
#16[g]	1:250:500:500	RT	24	38	99	19	96	n.d.	n.d.
#17[h]	1:250:500:500	RT	24	5	90	18	98	n.d.	n.d.

[a] Relative integral in the normalised ^{1}H NMR spectrum ($CDCl_3$, 400 MHz) of tertiary CHMe resonances due to polymer and dt-c5c versus unconsumed PO in the crude polymerisation mixture. [b] Relative integrals in the normalised ^{1}H NMR spectrum of tertiary CHMe resonances due to polymer versus dt-c5c in the crude polymerisation mixture. [c] Relative integrals in the normalised ^{1}H NMR spectrum ($CDCl_3$, 400 MHz) of tertiary CHMe resonances part of repeat units comprising R–S–S–R versus R–S–S_y-R links. [d] Relative integrals in the normalised ^{1}H NMR spectrum of resonances due to OSO and S_x versus other links in the precipitated polymer. [e]Determined by GPC (gel permeation chromatography) measurements conducted in THF with polystyrene calibration. [f] 1 eq. Ph_3NPh_3Cl:400 eq.PS: 400 eq. S with 50vol% toluene in Reference to Ref.[31] [g]Na was used as catalyst instead of Li. [h]K was used as catalyst instead of Li.

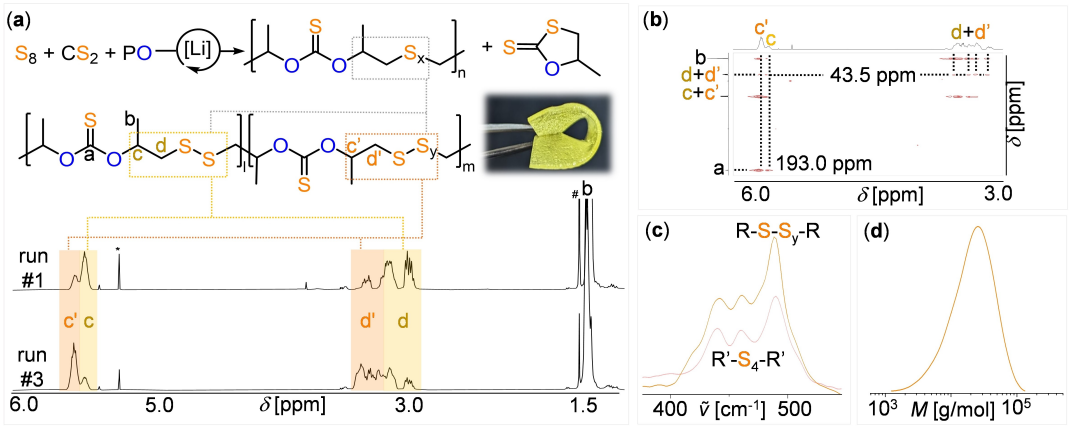

Figure 2. (a) Synthetic scheme, photograph of polymer film and overlaid ^{1}H NMR spectra ($CDCl_3$, 400 MHz) of polymers corresponding to Table 1 run #1 and #3. * Denotes residual DCM from purification. # residual H_2O. (b) ^{1}H-^{13}C HMBC NMR spectra of polymer corresponding to Table 1 run #1. (3) Zoom into the overlaid Raman spectra of polymer corresponding to Table 1 run #3 and a small molecule R'-S_4-R' standard. (d) Molar mass distribution of the copolymer corresponding to Table 1 run #1 as obtained by GPC (eluent: THF) with polystyrene calibration.

selectivity. Evidently, supplying additional S_8 is beneficial to improve polymer selectivity. Comparing the ^{1}H NMR spectra of the obtained copolymers showed that the tertiary CH resonances are always observed as two overlapping resonances centred around 5.64 and 5.72 ppm, and the latter becoming increasingly pronounced in copolymers obtained with higher initial S_8 loading. Employing enantiopure (R)-PO instead of racemic PO allows for deconvolution of the CH_2 ^{1}H NMR resonances adjacent to the S_x links in the precipitated polymers for which analogous sets of signals can be observed (ESI Figure S3). Comparing the Raman spectra of the precipitated polymers with small molecule standards for di- (R–S–S–R), tri- (R–S–S–S–R) and tetrasulfide (R–S–S–R) allowed us to draw some further conclusions about the S_x links (ESI Figure S12–15). At low sulfur loadings (run #5) disulfide links (sharp signal around $\tilde{\nu} = 507\ cm^{-1}$) were mostly formed, while at higher sulfur loadings (run #3) tetrasulfide links (Figure 2**(c)**) were predominant. As Raman spectroscopy clearly revealed more R–S–S_y–R ($y > 1$) polysulfide versus R–S–S–R disulfide links at higher sulfur loading, we assigned the ^{1}H NMR signal centred around 5.64 ppm to CH groups as part of repeat units containing R–S–S–R disulfide and the signal centred around 5.72 ppm to CH groups as part of repeat

© 2024 The Authors. Angewandte Chemie International Edition published by Wiley-VCH GmbH

15213773, 2024, 17, Downloaded from https://onlinelibrary.wiley.com/doi/10.1002/anie.202319810 by Universitaet Bayreuth, Wiley Online Library on [03/10/2024]. See the Terms and Conditions (https://onlinelibrary.wiley.com/terms-and-conditions) on Wiley Online Library for rules of use; OA articles are governed by the applicable Creative Commons License

units containing R–S–S_y–R polysulfide links. By peak deconvolution in each case, the R–S–S–R to R–S–S_y–R ratios were found to change from 89:11 to 15:85 at low to high sulfur loadings. Furthermore, for run #4 we observed unreacted elemental sulfur to be left in the crude reaction mixture indicating that there appears to be an upper limit to how much sulfur can be incorporated into the R–S–S_y–R links which is reminiscent of Penczek and Duda's original findings.[29] Next, we assessed the effects of different S_8 to CS_2 loading ratios (run #9–#12) and found excellent sequence selectivities and similar molar masses in each case. However, polymer selectivity was somewhat decreased to 77 % for lower CS_2 loadings. Decreasing the catalyst loading at a fixed monomer ratio leads to larger obtained molar masses of $M_w = 45$ kDa (run #13), though the highest achievable molar mass appears to be limited. A decrease of the catalyst loading (run #14) does not lead to further increase of the molar mass beyond 45 kDa. Accordingly, GPC analysis of aliquots removed at regular time intervals revealed increasing molar masses with conversion, reaching a plateau in the high conversion regime (ESI Figure S19). This could be due to the formation of cyclic polymers although the BnO end group could be identified, hence the copolymers are also likely linear chains. Nevertheless, molar masses between 10–50 kDa seems to be typical for S_8 ROCOP (and ROTERP), as reproducing a literature known S_8/PS ROCOP[31] at a comparable loading (run #15, compared to runs #2–4) gave copolymers with similar molar masses. Employing NaOBn or KOBn (run #16–17) instead of the LiOBn catalyst led to significantly slower indicating that Li acts as a true catalyst rather than a mere spectator counteraction to the chain end. Looking at the combined results from Table 1 no clear conclusion can be drawn how the monomer feed ratio affects the observed linkage selectivity due to the overall high selectivity observed.

We also investigated the suitability of other epoxides than PO to our new methodology (ESI Section S6) and found a range of monosubstituted and alicyclic epoxides (Figure 3) to likewise undergo ROTERP with S_8 and CS_2 (Table 2) which we examined at the monomer feeds and conditions of Table 1 **run #1**.

Moving to monosubstituted epoxides with longer alkyl chains, such as butylene oxide (BO) and 1,2-decylene oxide (DO), gave similar results as the ROTERP of PO under the same conditions, producing a poly(OSO-*alt*-S_x) with head-to-head-*alt*-tail-to-tail regioselectivity. Compared to the T_g of the PO terpolymer (4 °C), the BO terpolymer shows a slightly higher T_g of 19 °C while the DO terpolymer shows a slightly lower T_g of −12 °C. The ROTERP of cyclohexene oxide (CHO) yielded a material with an increased T_g of 70 °C at a somewhat reduced linkage selectivity compared to the monosubstituted epoxides. This is in line with findings by Werner and Komber et al. who observed reduced linkage selectivity in the parent CS_2/CHO ROCOP.[35] Glycidyl ethers can also be terpolymerised with almost quantitative linkage selectivity and excellent OSO-*alt*-S_x (head-to-head-*alt*-tail-to-tail) selectivity, yielding materials with a T_g below room temperature (−12 °C) for the ethyl derivative EGE and above room temperature (+30 °C) for the phenyl derivative PGE. Lastly, terpolymerisation of styrene oxide (SO), which is an intrinsically challenging epoxide in ROCOP catalysis, could also be achieved although maximum conversion and molar mass were reduced (Table 2) resulting in a T_g *of* 12 °C. Multinuclear NMR analysis revealed a regio-random microstructure as opposed to a head-to-head-*alt*-tail-to-tail sequence although OSO links could also be identified.[46] It should be noted that the T_g's should be considered with caution due to the differences in molecular weight, regioselectivity, linkage errors and length of polysulfide chain. In fact, surveying different PO terpolymers from Table 1 by DSC (see ESI Figure S20) shows that the T_g can vary by 20 °C implying that further investigations

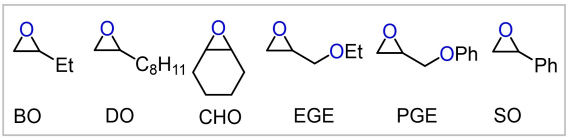

Figure 3. Epoxides explored for ROTERP with S_8 and CS_2.

Table 2: Reaction conditions and molecular characteristics of the polymers obtained by ROTERP of various epoxides with S_8 and CS_2.

Epoxide	t	Conv. [%][a] -	Polmer [%][b]	-SS- [%][c]	Linkage select. [%][d]	M_w [kDa][e]	$Đ$[e]	T_g [°C][g]	$T_{d,5\%}$ [°C]
PO	3 h	96	84	70	98	20	1.7	4	160
BO	3 w	60	90	67	97	16	1.7	19	160
DO	2 d	63	75	70	96	12	1.4	−12	170
CHO	2 d	47	66	42	82	15	1.7	70	150
EGE	2 d	95	73	54	99	19	1.6	−13	175
PGE	2 d	62	68	50	98	9	1.4	30	180
SO	1 w	14	52	n.d.	n.d. [f]	4	1.3	13	150

ROTERP conducted at 30 °C with 1 eq. LiOBn: 250 eq. Epoxide: 250 eq. CS_2: 125 eq. $^1/_8$ S_8. [a] Relative peak integrals in the normalised ^{1}H NMR spectrum ($CDCl_3$, 400 MHz) of tertiary CHMe resonances due to polymer and cyclic dithiocarbonate versus unconsumed epoxide. [b] Relative integrals in the normalised ^{1}H NMR spectrum of tertiary CHMe resonances due to polymer versus cyclic dithiocarbonate. [c] Relative integral in the normalised ^{1}H NMR spectrum ($CDCl_3$, 400 MHz) of tertiary CHMe resonances part of repeat units comprising –S–S– versus –S–S_y– links. [d] Relative integrals in the normalised ^{1}H NMR spectrum of tertiary CHMe resonances due to OSO and S_x versus other links. [e] Determined by GPC (gel permeation chromatography) measurements conducted in THF with a narrow polystyrene standard. [f] Linkage selectivity could not be determined due to complexity of the spectrum. [g] Determined by DSC from second heating curve at 10 K/min.

© 2024 The Authors. Angewandte Chemie International Edition published by Wiley-VCH GmbH

15213773, 2024, 17, Downloaded from https://onlinelibrary.wiley.com/doi/10.1002/anie.202319810 by Universitaet Bayreuth, Wiley Online Library on [03/10/2024]. See the Terms and Conditions (https://onlinelibrary.wiley.com/terms-and-conditions) on Wiley Online Library for rules of use; OA articles are governed by the applicable Creative Commons License

are required to make definite statements on structure–property relationships. In terms of $T_{d,5\%}$ these range between 150 and 180 °C as presented in Table 2. Again, the $T_{d,5\%}$ vary by ca. 10 °C for PO terpolymers of different composition from Table 1 (see ESI Figure S21) limiting statements about structure–property relationships at the current stage.

Next, we tried to elucidate the polymerisation mechanism with quantum chemical studies to understand the origin of sequence selectivity as well as how sulfur centres get distributed along the polymer chain. For all DFT-calculations presented in the following it was tried to account for all types of more probable coordination modes around Li (including dinuclear species) and to explore conformational spaces of each species as exhaustive as possible, for details see ESI Section S8. In the following, for each intermediate of the catalytic cycle only the species with the lowest Gibbs free energy is discussed. Figure 4**(a)** shows a mechanistic hypothesis which makes sense from a thermodynamic point of view as Gibbs free energy decreases along any polymer growth step. Our mechanistic hypothesis starts from a lithium alkoxide **A** that serves as the energetic reference at 0.0 kJ/mol. **A** generates a lithium dithiocarbonate **DTC** by addition to CS_2 in step (i). PO ring opening by **DTC** in step (ii) leads to a lithium alkoxide **A'** that rearranges via an intermediate **I** in step (iii) into a lithium thiolate **T** in step (iv), analogous to reports by Komber and Werner et al.[35] Elimination of alkoxide **A** from the intermediate **I** in step (v) instead of O/S exchange yields the cyclic dithiocarbonate dt-c5c by-product. In the next step (vi) or (vi'), S_8 or CS_2 is inserted to form a lithium oligosulfide **S** in (vi) or a lithium trithiocarbonate **TT** in (vi'), whereas the latter case appears to occur substantially less given the observed sequence selectivity. As it is well established that S_8 forms a distribution of anionic oligosulfides upon ring opening, **S** likely corresponds to a distribution of lithium oligosulfides R-S_x-Li with a maximum clearly below the initial $x = 9$.[47] Formation of longer polysulfides is thermodynamically unfeasible below the floor temperature of elemental sulfur, as previously shown by Penczek and Duda.[29] Thereafter PO insertion in (vii) regenerates the alkoxide **A** to close the cycle.

As PO or S_8 are not expected to react with the alkoxides **A** or **A'** for kinetic (PO) or thermodynamic (S_8) reasons and as PO ring opening by lithium thiolates **T** must be kinetically disfavoured compared to an addition to CS_2 (nucleophilic substitution vs addition to a carbonyl centre), the question remains what causes sequence selectivity towards an S_8 incorporation over trithiiocarbonate formation in (vi).[48] Elucidating the reaction kinetics, we followed the PO consumption (ESI Figure S22, Figure 5**(a)**) of a ROTERP by ^{1}H NMR at an initial loading of LiOBn:PO:CS_2:S = 1:500:500:70. This revealed a 0th order dependence of the ROTERP with respect to S_8. After the completion of ROTERP the reaction switches to CS_2/PO ROCOP which is maintaining the rate of PO consumption. This indicates that CS_2/PO ROCOP and S_8/CS_2/PO ROTERP likely have the same rate-determing step which supposedly is (ii) as epoxide ring-opening typically represents the slowest reaction step(s) in such reactions, as mentioned before.[48] Furthermore, from these results, one would assume that S_8 insertion by **T** is much faster than the other reaction steps.

Considering the thermodynamics of S_8 versus CS_2 insertion by **T** (Figure 5**(b)**), DFT calculations show that the latter is more favourable from a thermodynamic point of view. Assuming an also rather high epoxide ring opening barrier for (vi) and (vi'), this would imply that there is an equilibration between **S** and **TT** (with significant amounts of **TT** in the mixture) and the observed sequence selectivity must have kinetic reasons. This is in fact confirmed by computations of the propagation barriers revealing lower activation energies for the lithium oligosulfide **S** inserting into PO ($\Delta G^{\ddagger} = 96.5$ to 134.2 kJ/mol depending on the S_x length) than for the trithiocarbonate **TT** ($\Delta G^{\ddagger} = 147.6$ kJ/mol). In other words, lithium oligosulfide **S** are better nucleophiles than lithium trithiocarbonates **TT**. It is worth mentioning that the most preferred transition states for both (vi) and (vi') are zwitterionic in the sense that they occur via chain-end dissociation away from the lithium centre and subsequent attack of the CH_2 group of PO in an almost 180°

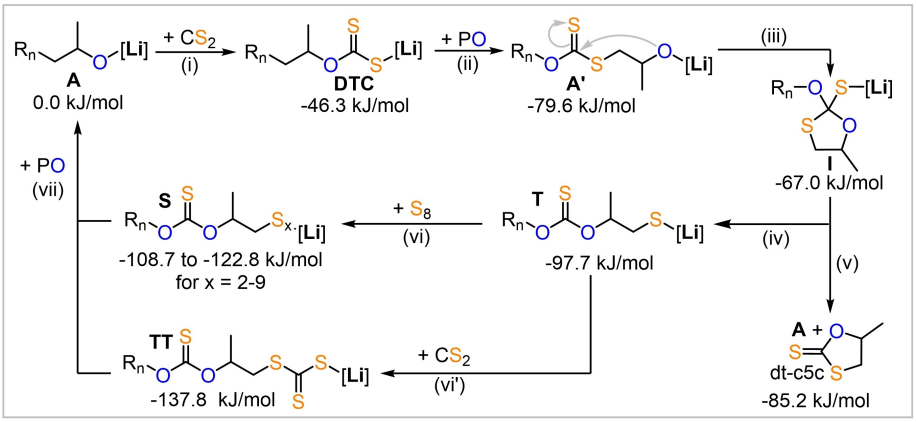

Figure 4. (a) Mechanistic hypothesis for S_8/CS_2/PO ROTERP. Gibbs free energies associated with the respective intermediates below the labels was assessed from a series of structures involving different Li coordination modi which are outlined in the Supporting Information (ESI Section S8).

© 2024 The Authors. Angewandte Chemie International Edition published by Wiley-VCH GmbH

15213773, 2024, 17, Downloaded from https://onlinelibrary.wiley.com/doi/10.1002/anie.202319810 by Universitaet Bayreuth, Wiley Online Library on [03/10/2024]. See the Terms and Conditions (https://onlinelibrary.wiley.com/terms-and-conditions) on Wiley Online Library for rules of use; OA articles are governed by the applicable Creative Commons License

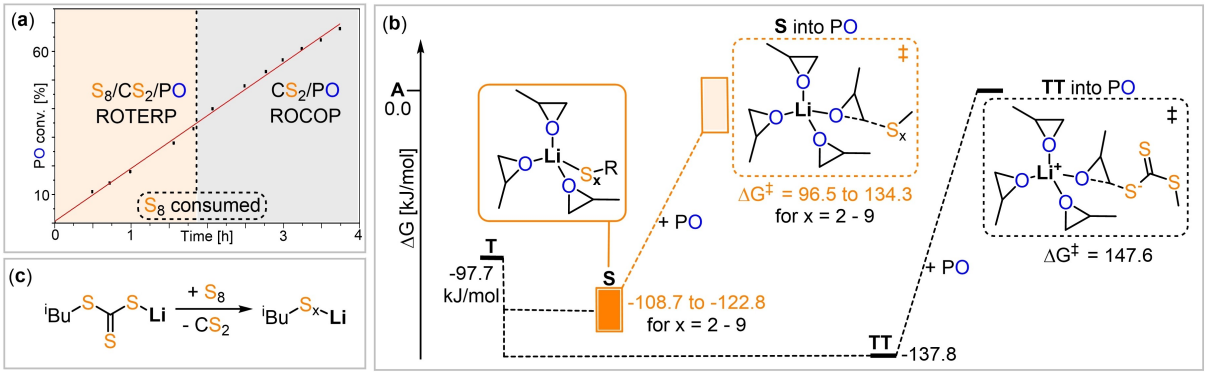

Figure 5. (a) Kinetic reaction traces of S_8/CS_2/PO ROTERP switching into CS_2/PO ROCOP after S_8 consumption. (b) Computed PO ring opening barriers by **S** and **TT**. (c) Small molecule model reaction substantiating the reversibility of CS_2 insertion.

angle with respect to the broken bond, which is the preferred constellation to the C-atom in S_N2 reactions. A mechanistic alternative would be a bimetallic transition state; this was also tried and leads to the same trend in Gibbs free activation energies for the reactions of **TT** versus **S** (see ESI Section S8) but is generally disfavoured with respect to the zwitterionic pathways. If propagation from **S** is kinetically favoured but formation of **TT** is thermodynamically favoured, CS_2 insertion must be reversible so that **TT** can transform into **S** and the kinetically more viable pathway can be accessed to form the observed Poly(OSO-*alt*-S_x) sequence. Seeking to validate this experimentally we undertook a small molecule model reaction (Figure 5**(c)**) in which we exposed a lithium thiolate, ^{i}BuSLi, first to CS_2 in d_8-THF to quantitatively form the corresponding lithium trithiocarbonate ^{i}BuS(C=S)SLi and thereafter added elemental sulfur. Indeed, ^{1}H NMR analysis of the reaction mixture (ESI Figure S27) reveals the partial dissapearance of the signals of ^{i}BuS(C=S)SLi and the appearance of new signals which can be assigned to S_8 insertion products by comparison to the stand-alone reaction between ^{i}BuSLi and S_8. This unambigously proves that CS_2 insertion is reversible and that **TT** can transform into **S** to access the kinetically favourable propagation pathway. Furthermore we infer that this effective promotion of propagation due to the presence of S_8 in reaction mixtures effectively limits the lifetime of **T** which in principle can also produce dt-c5c by-products by reversion of step (iv) and this helps to explain the improvement in polymer selectivity of S_8/CS_2/PO ROTERP compared to CS_2/PO ROCOP.

In terms of overall polymerisation thermodynamics, computational assessment of the Gibbs free energy of formation of possible repeat units from CS_2/PO versus S_8/CS_2/PO is shown in Figure 6. Here formation of the poly(OSO-*alt*-S_x) sequence from S_8/CS_2/PO ROTERP is more exergonic than the poly(OSO-*alt*-SSS) sequence from CS_2/PO ROCOP irrespective of the length of S_x. Interestingly there is a shallow minimum for sequences with tetrasulfide S_4 links which could also be experimentally identified as pronounced links in the polymers by Raman spectroscopy (see above). This shows that S_8/CS_2/PO

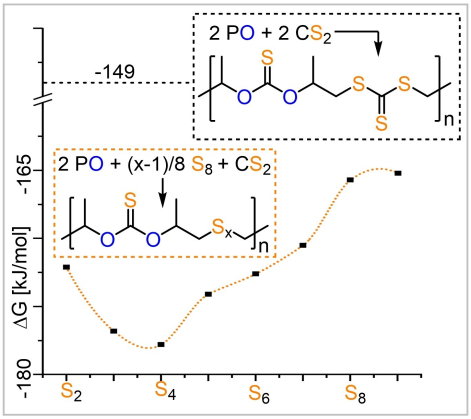

Figure 6. Gibbs free energy of formation for links from CS_2/PO ROCOP versus S_8/CS_2/PO ROTERP with different S_x length.

ROTERP is also thermodynamically favoured to occur over CS_2/PO ROCOP.

A final open question concerns whether the R-S_x-R links remain reactive after formation in (vii) which is a likely hypothesis due to the chemical similarity of neutral R-S_x-R to S_8. As we can spectroscopically identify the disulfide R–S–S–R and oligosulfide R–S–S_y–R links, we used these as an experimental handle. ^{1}H NMR aliquot analysis of a ROTERP at a loading of LiOBn:PO:CS_2:S = 1:500:500:70 revealed that the proportion of R–S–S–R and R–S–S_y–R links changes throughout polymerisation. As can be seen in Figure 7**(a)**, R–S–S_y–R polysulfide links were formed at an early stage of the polymerisation and these slowly declined at above 18 % PO conversion until they could no longer be observed at 57 % PO conversion. This implies that the polysulfide R–S–S_y–R links remain reactive and undergo sulfur redistribution. Seeking to confirm this hypothesis we added a preformed S_8/CS_2/PO terpolymer (Table 1 run #2) containing R–S–S_y–R links to a ROCOP of CS_2/PO. As thiolate intermediates are formed in ROCOP, these must react with the R–S–S_y–R links to eventually reshuffle the sulfur centres into new disulfide R–S–S–R links–which is indeed what we observed, see Figure 6**(b)**. Furthermore, we recognised a slight increase of M_w from 23 to 35 kDa (ESI

© 2024 The Authors. Angewandte Chemie International Edition published by Wiley-VCH GmbH

15213773, 2024, 17, Downloaded from https://onlinelibrary.wiley.com/doi/10.1002/anie.202319810 by Universitaet Bayreuth, Wiley Online Library on [03/10/2024]. See the Terms and Conditions (https://onlinelibrary.wiley.com/terms-and-conditions) on Wiley Online Library for rules of use; OA articles are governed by the applicable Creative Commons License

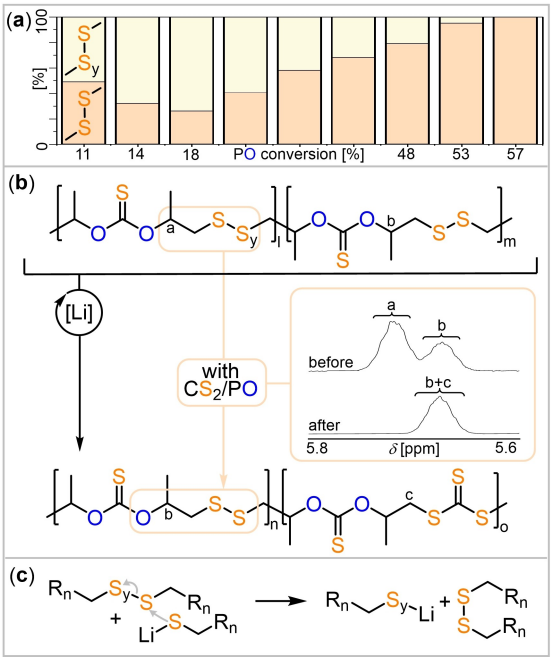

Figure 7. (a) Evolution of di and polysulfide link distribution during ROTERP of S_8/CS_2/PO at 1 eq. LiOBn : 500 eq. PO: 500 eq. CS_2: 70 eq S. (b) Tranformation of R–S–S_y-R links in a ROTERP polymer into R–S–S_y-R links when CS_2/PO ROCOP occurs via in situ formed thiolates. (c) Mechanistic hypothesis concerning the reshuffling of sulfur centres exemplified with the intermolecular formation of R–S–S–R from R–S–S_y-R links.

Figure S28), suggesting that the reshuffling process reactivates the ROTERP chains to insert further monomer. We therefore suggest a reshuffling pathway as shown in Figure 7**(c)**. Here R–S–S_y–R links are susceptible to nucleophilic attack by thiolate intermediates, alike reaction step (vi) in Figure 4, in which now R–S–S_y–R links are cleaved in place of S_8.

Having learned that the polysulfide R–S–S_y–R links remain reactive after formation, we were intrigued to see if these could serve as sites for the crosslinking of multiple chains. Inspired by the precedence concerning base-mediated thiol-disulfide exchange,[49] we attempted crosslinking of the copolymers in situ after ROTERP by addition of a tetrafunctional thiol (pentaerythritol tetrakis(3-mercaptopropionate), ca. 25 wt % versus polymer) in air. We assumed that the anionic lithium chain ends could act as a base to catalyse the thiol-disulfide exchange reaction. Indeed, while the diluted ROTERP reaction mixture (Table 1 run #14) at full PO consumption was freely flowing, it turned into a stable network or gel, which resided at the top of the reaction vial after inversion, upon addition of the crosslinker (Figure 8). Interestingly, during crosslinking, we recognised the evolution of a gas, which could be identified as carbonyl sulfide (IR $\tilde{\nu}$ (COS) = 2060 cm^{-1}, ESI Figure S59); a mechanistic hypothesis of the crosslinking process is shown in the Supporting Information (Scheme S6). The Raman spectrum of the crosslinked material clearly shows the presence of polysulfide R-S_x-R groups ($\tilde{\nu}$ = 350 - 550 cm^{-1}) but no SH functionalities ($\tilde{\nu}$ = *2500–2600* cm^{-1}) (ESI Figure S66–67). We infer that this is due oxidative coupling of thiols to R–S–S–R disulfides as part of the crosslinking process in air.

Drying of the gel yielded a rubbery material (T_g = −2 °C) with a degradation profile that shows a similar onset of degradation ($T_{d,5\%}$ ca. 160 °C) as the linear parent polymer but some higher thermal stability above 200 °C (ESI Figure S63). Comparative rheological analysis of linear and crosslinked polymer shows an increasing gap (G'–G'' with G' > G'') between the elastic (G') and viscous (G'') component, further substantiating successful crosslinking (ESI Figure S64). Importantly, the rheological profile of the material in the amplitude sweep test was affected by the amount of tetra-thiol crosslinker, which suggests some tunability of the mechanical properties of our materials (ESI Figure S65). The crosslinked material is yellow and optically transparent (see below), shows a good refractive index (RI = 1.63) and an Abbe number of 30, potentially rendering it interesting for optical applications.[13] Furthermore surfaces can be easily covered with it via dip-coating (ESI Figure S68).

Exposing the dried gel materials to DCM (a good solvent for the parent polymer) resulted in swelling but not dissolution, as expected. Determination of the sol-gel fraction suggested that the gel contained 85 wt % of the initial material while the soluble portion contained the dt-c5c by-product from the ROTERP stage (ESI Figure S69). Although covalent network structures (usually) impede solution processing, we thought that here thermal reprocessing could be feasible due to the dynamic nature of the polysulfide bonds. Indeed, hot-pressing of the granulated material could be achieved at 80 °C to yield a self-standing

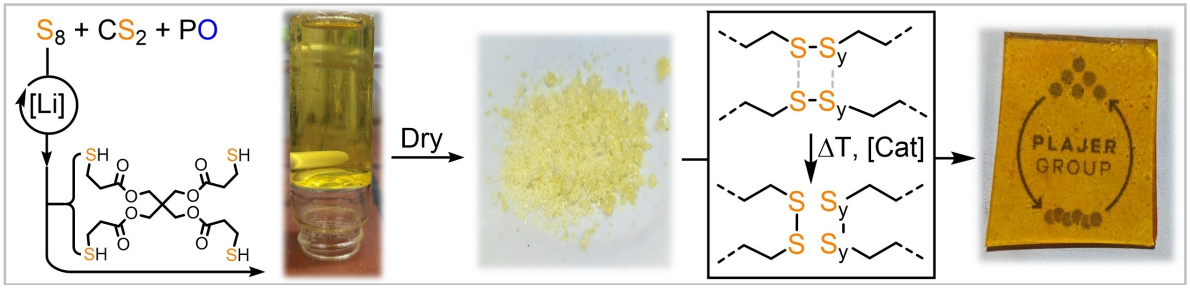

Figure 8. Gelation of diluted ROTERP reaction mixture with tetrafunctional thiol and thermal reprocessing of dried network via polysulfide reaction.

© 2024 The Authors. Angewandte Chemie International Edition published by Wiley-VCH GmbH

15213773, 2024, 17, Downloaded from https://onlinelibrary.wiley.com/doi/10.1002/anie.202319810 by Universitaet Bayreuth, Wiley Online Library on [03/10/2024]. See the Terms and Conditions (https://onlinelibrary.wiley.com/terms-and-conditions) on Wiley Online Library for rules of use; OA articles are governed by the applicable Creative Commons License

and homogeneous film (see Figure 7). Adding an extra Lewis base such as NEt_3 to the network promoted faster reprocessing at a given temperature and pressure (ESI Figure S60).[50,51] The possible thermal reprocessing further implies that these disulfide-crosslinked materials should be degradable by similar exchange reactions with small molecules. Accordingly, treatment of a crosslinked sample, which remained stable in DCM for weeks, with ^{i}BuSH and NEt_3 caused break down of the network within minutes (see supplementary video in the ESI), a property which is for example also useful in the context of thiol sensing.[52]

Conclusions

In conclusion, we introduced a ring-opening terpolymerisation (ROTERP) process to produce sulfur-containg polymer materials from commercially relevant epoxides, carbon disulfide and elemental sulfur waste. The process requires trace amounts of a cheap lithium alkoxide catalyst and occurs without external heating. Mechanistic investigations showed that S_8 insertion leads to more facile propagation thereafter which enables the sequence selectivity. As the R–S–S_y–R links in the polymer remain susceptible towards nucleophilic attack by thiolate intermediates one can crosslink the chains in situ with multifunctional thiols producing reprocessable and degradable networks. Our report demonstrates how mechanistic understanding in alkali metal catalysis can turn waste S_8 with commercially viable comonomers into complex polymers with tunable properties, reprocessability and degradability.

Acknowledgements

The VCI is acknowledged for a Liebig Fellowship for A. J. P and a Ph.D. scholarship for C.G. Dr. Patrick Pröhm is thanked for valuable consultation. Open Access funding enabled and organized by Projekt DEAL.

Conflict of Interest

There are no conflicts of interest.

Data Availability Statement

The data that support the findings of this study are available in the supplementary material of this article.

Keywords: sulfur waste · ring-opening polymerisation · degradable polymers · alkali metal catalysis

[1] T.-J. Yue, W.-M. Ren, X.-B. Lu, *Chem. Rev.* **2023**, 10.1021/acs.chemrev.3c00437.
[2] P. Yuan, Y. Sun, X. Xu, Y. Luo, M. Hong, *Nat. Chem.* **2022**, *14*, 294–303.
[3] Y. Wang, M. Li, J. Chen, Y. Tao, X. Wang, *Angew. Chem. Int. Ed.* **2021**, *60*, 22547–22553.
[4] X.-F. Zhu, G.-W. Yang, R. Xie, G.-P. Wu, *Angew. Chem. Int. Ed.* **2022**, *61*, e202115189.
[5] T.-J. Yue, B.-H. Ren, W.-J. Zhang, X.-B. Lu, W.-M. Ren, D. J. Darensbourg, *Angew. Chem. Int. Ed.* **2021**, *60*, 4315–4321.
[6] J. Zhang, T. Bai, W. Liu, M. Li, Q. Zang, C. Ye, J. Z. Sun, Y. Shi, J. Ling, A. Qin, B. Z. Tang, *Nat. Commun.* **2023**, *14*, 3524.
[7] Y.-L. Su, L. Yue, H. Tran, M. Xu, A. Engler, R. Ramprasad, H. J. Qi, W. R. Gutekunst, *J. Am. Chem. Soc.* **2023**, *145*, 13950–13956.
[8] R. A. Smith, G. Fu, O. McAteer, M. Xu, W. R. Gutekunst, *J. Am. Chem. Soc.* **2019**, *141*, 1446–1451.
[9] Y. Zhu, M. Li, Y. Wang, X. Wang, Y. Tao, *Angew. Chem. Int. Ed.* **2023**, *62*, e202302898.
[10] Y. Xia, X. Yue, Y. Sun, C. Zhang, X. Zhang, *Angew. Chem. Int. Ed.* **2023**, *62*, e202219251.
[11] F. H. Sobotta, M. T. Kuchenbrod, F. V. Gruschwitz, G. Festag, P. Bellstedt, S. Hoeppener, J. C. Brendel, *Angew. Chem. Int. Ed.* **2021**, *60*, 24716–24723.
[12] T. Lee, P. T. Dirlam, J. T. Njardarson, R. S. Glass, J. Pyun, *J. Am. Chem. Soc.* **2022**, *144*, 5–22.
[13] K.-S. Kang, C. Olikagu, T. Lee, J. Bao, J. Molineux, L. N. Holmen, K. P. Martin, K.-J. Kim, K. H. Kim, J. Bang, V. K. Kumirov, R. S. Glass, R. A. Norwood, J. T. Njardarson, J. Pyun, *J. Am. Chem. Soc.* **2022**, *144*, 23044–23052.
[14] H. Yang, J. Huang, Y. Song, H. Yao, W. Huang, X. Xue, L. Jiang, Q. Jiang, B. Jiang, G. Zhang, *J. Am. Chem. Soc.* **2023**, *145*, 14539–14547.
[15] W. Cao, F. Dai, R. Hu, B. Z. Tang, *J. Am. Chem. Soc.* **2020**, *142*, 978–986.
[16] T. Tian, R. Hu, B. Z. Tang, *J. Am. Chem. Soc.* **2018**, *140*, 6156–6163.
[17] J. Zhang, Q. Zang, F. Yang, H. Zhang, J. Z. Sun, B. Z. Tang, *J. Am. Chem. Soc.* **2021**, *143*, 3944–3950.
[18] W. J. Chung, J. J. Griebel, E. T. Kim, H. Yoon, A. G. Simmonds, H. J. Ji, P. T. Dirlam, R. S. Glass, J. J. Wie, N. A. Nguyen, B. W. Guralnick, J. Park, Á. Somogyi, P. Theato, M. E. Mackay, Y.-E. Sung, K. Char, J. Pyun, *Nat. Chem.* **2013**, *5*, 518–524.
[19] J. Jia, J. Liu, Z.-Q. Wang, T. Liu, P. Yan, X.-Q. Gong, C. Zhao, L. Chen, C. Miao, W. Zhao, S. (Diana) Cai, X.-C. Wang, A. I. Cooper, X. Wu, T. Hasell, Z.-J. Quan, *Nat. Chem.* **2022**, *14*, 1249–1257.
[20] P. Yan, W. Zhao, F. McBride, D. Cai, J. Dale, V. Hanna, T. Hasell, *Nat. Commun.* **2022**, *13*, 4824.
[21] X. Wu, J. A. Smith, S. Petcher, B. Zhang, D. J. Parker, J. M. Griffin, T. Hasell, *Nat. Commun.* **2019**, *10*, 647.
[22] J. Bao, K. P. Martin, E. Cho, K.-S. Kang, R. S. Glass, V. Coropceanu, J.-L. Bredas, W. O. Jr. Parker, J. T. Njardarson, J. Pyun, *J. Am. Chem. Soc.* **2023**, *145*, 12386–12397.
[23] M. P. Crockett, A. M. Evans, M. J. H. Worthington, I. S. Albuquerque, A. D. Slattery, C. T. Gibson, J. A. Campbell, D. A. Lewis, G. J. L. Bernardes, J. M. Chalker, *Angew. Chem. Int. Ed.* **2016**, *55*, 1714–1718.
[24] J. M. Scheiger, M. Hoffmann, P. Falkenstein, Z. Wang, M. Rutschmann, V. W. Scheiger, A. Grimm, K. Urbschat, T. Sengpiel, J. Matysik, M. Wilhelm, P. A. Levkin, P. Theato, *Angew. Chem. Int. Ed.* **2022**, *61*, e202114896.
[25] J. J. Griebel, S. Namnabat, E. T. Kim, R. Himmelhuber, D. H. Moronta, W. J. Chung, A. G. Simmonds, K.-J. Kim, J. van der Laan, N. A. Nguyen, E. L. Dereniak, M. E. Mackay, K. Char, R. S. Glass, R. A. Norwood, J. Pyun, *Adv. Mater.* **2014**, *26*, 3014–3018.
[26] K.-S. Kang, A. Phan, C. Olikagu, T. Lee, D. A. Loy, M. Kwon, H. Paik, S. J. Hong, J. Bang, W. O. Parker Jr., M. Sciarra,

© 2024 The Authors. Angewandte Chemie International Edition published by Wiley-VCH GmbH

15213773, 2024, 17, Downloaded from https://onlinelibrary.wiley.com/doi/10.1002/anie.202319810 by Universitaet Bayreuth, Wiley Online Library on [03/10/2024]. See the Terms and Conditions (https://onlinelibrary.wiley.com/terms-and-conditions) on Wiley Online Library for rules of use; OA articles are governed by the applicable Creative Commons License

A. R. de Angelis, J. Pyun, *Angew. Chem. Int. Ed.* **2021**, *60*, 22900–22907.
[27] H. Mutlu, E. B. Ceper, X. Li, J. Yang, W. Dong, M. M. Ozmen, P. Theato, *Macromol. Rapid Commun.* **2019**, *40*, 1800650.
[28] S. Penczek, R. Ślazak, A. Duda, *Nature* **1978**, *273*, 738–739.
[29] S. Penczek, A. Duda, *Phosphorus Sulfur Silicon Relat. Elem.* **1991**, *59*, 47–62.
[30] S. Penczek, A. Duda, *Pure Appl. Chem.* **1981**, *53*, 1679–1687.
[31] W.-M. Ren, J.-Y. Chao, T.-J. Yue, B.-H. Ren, G.-G. Gu, X.-B. Lu, *Angew. Chem. Int. Ed.* **2022**, *61*, e2021159.
[32] M. I. Childers, J. M. Longo, N. J. Van Zee, A. M. LaPointe, G. W. Coates, *Chem. Rev.* **2014**, *114*, 8129–8152.
[33] J. Herzberger, K. Niederer, H. Pohlit, J. Seiwert, M. Worm, F. R. Wurm, H. Frey, *Chem. Rev.* **2016**, *116*, 2170–2243.
[34] A. J. Plajer, C. K. Williams, *Angew. Chem. Int. Ed.* **2022**, *61*, e202104495.
[35] J. Diebler, H. Komber, L. Häußler, A. Lederer, T. Werner, *Macromolecules* **2016**, *49*, 4723–4731.
[36] S. Rupf, P. Pröhm, A. J. Plajer, *Chem. Sci.* **2022**, *13*, 6355–6365.
[37] C. Fornacon-Wood, B. R. Manjunatha, M. R. Stühler, C. Gallizioli, C. Müller, P. Pröhm, A. J. Plajer, *Nat. Commun.* **2023**, *14*, 4525.
[38] T. M. McGuire, A. Buchard, *Polym. Chem.* **2021**, *12*, 4253–4261.
[39] M. Luo, X.-H. Zhang, D. J. Darensbourg, *Macromolecules* **2015**, *48*, 5526–5532.
[40] G. Feng, X. Feng, X. Liu, W. Guo, C. Zhang, X. Zhang, *Macromolecules* **2023**, *56*, 6798–6805.
[41] L.-Y. Wang, G.-G. Gu, B.-H. Ren, T.-J. Yue, X.-B. Lu, W.-M. Ren, *ACS Catal.* **2020**, *10*, 6635–6644.
[42] D. K. Tran, A. N. Braaksma, A. M. Andras, S. K. Boopathi, D. J. Darensbourg, K. L. Wooley, *J. Am. Chem. Soc.* **2023**, *145*, 18560–18567.
[43] C. Hardy, G. Kociok-Köhn, A. Buchard, *Chem. Commun.* **2022**, *58*, 5463–5466.
[44] A. J. Plajer, *ChemCatChem* **2022**, *14*, e202200867.
[45] L. J. Dodd, Ö. Omar, X. Wu, T. Hasell, *ACS Catal.* **2021**, *11*, 4441–4455.
[46] G.-P. Wu, S.-H. Wei, W.-M. Ren, X.-B. Lu, B. Li, Y.-P. Zu, D. J. Darensbourg, *Energy Environ. Sci.* **2011**, *4*, 5084–5092.
[47] R. Steudel, *Chemie der Nichtmetalle: Synthesen - Strukturen - Bindung–Verwendung*, Walter De Gruyter, **2013**.
[48] P. Deglmann, S. Machleit, C. Gallizioli, S. M. Rupf, A. J. Plajer, *Catal. Sci. Technol.* **2023**, *13*, 2937–2945.
[49] M. Pepels, I. Filot, B. Klumperman, H. Goossens, *Polym. Chem.* **2013**, *4*, 4955–4965.
[50] S. Nevejans, N. Ballard, J. I. Miranda, B. Reck, J. M. Asua, *Phys.l Chem. Chem. Phys.* **2016**, *18*, 27577–27583.
[51] S. J. Tonkin, C. T. Gibson, J. A. Campbell, D. A. Lewis, A. Karton, T. Hasell, J. M. Chalker, *Chem. Sci.* **2020**, *11*, 5537–5546.
[52] B. Klemm, A. Roshanasan, I. Piergentili, J. H. van Esch, R. Eelkema, *J. Am. Chem. Soc.* **2023**, *145*, 39, 21222–21230.

Manuscript received: December 22, 2023
Accepted manuscript online: February 29, 2024
Version of record online: March 18, 2024

© 2024 The Authors. Angewandte Chemie International Edition published by Wiley-VCH GmbH

15213773, 2024, 17, Downloaded from https://onlinelibrary.wiley.com/doi/10.1002/anie.202319810 by Universitaet Bayreuth, Wiley Online Library on [03/10/2024]. See the Terms and Conditions (https://onlinelibrary.wiley.com/terms-and-conditions) on Wiley Online Library for rules of use; OA articles are governed by the applicable Creative Commons License